Formation and cell translocation of carbon nanotube-fibrinogen protein corona

Ran Chen,[1] Slaven Radic,[1] Poonam Choudhary,[1] Kimberley G. Ledwell,[1] George Huang,[1] Jared M. Brown,[2] and Pu Chun Ke[1,a)]
[1]*Nano-Biophysics and Soft Matter Laboratory, COMSET, Clemson University, Clemson, South Carolina 29634, USA*
[2]*Department of Pharmacology & Toxicology, East Carolina University, Greenville, North Carolina 27834, USA*

(Received 11 August 2012; accepted 17 September 2012; published online 27 September 2012)

The binding of plasma fibrinogen with both single-walled and multi-walled carbon nanotubes (SWNTs and MWNTs) has been examined. Specifically, our absorbance study indicated that MWNTs were coated with multi-layers of fibrinogen to render a "hard protein corona," while SWNTs were adsorbed with thin layers of the protein to precipitate out of the aqueous phase. In addition, static quenching as a result of energy transfer from fluorescently labeled fibrinogen to their nanotube substrates was revealed by Stern-Volmer analysis. When exposed to HT-29 cells, the nanotubes and fibrinogen could readily dissociate, possibly stemming from their differential affinities for the amphiphilic membrane bilayer. © *2012 American Institute of Physics*. [http://dx.doi.org/10.1063/1.4756794]

Carbon-based nanomaterials have been studied extensively over the past two decades for their unique physical properties and vast potential in electronics, imaging, sensing, biotechnology, and environmental remediation. Carbon nanotubes (CNTs), a major class of carbon-based nanomaterials, are especially attractive for biological and medicinal applications owing to their large surface area, high aspect ratio, and simplicity for accommodating chemical groups and drug loads.[1] However, integrating carbon nanomaterials with biological systems must first address the inherently poor solubility and biocompatibility of the engineered materials, on molecular, cellular, and whole organism levels.[2,3]

The solubility and biocompatibility of carbon-based nanomaterials may be afforded or enhanced through specific surface functionalization or nonspecific adsorption of proteins, lipids, amino acids, and nucleic acids.[4–8] Alternatively to such purposeful surface modifications, nanoparticles (NPs) voluntarily assume the form of a NP-protein "corona" upon entering living systems,[9] resulting from their surface adsorption by plasma proteins and other biomolecular species. Naturally, understanding the formation of NP-protein corona has become a focused area of study due to its great relevance to delineating the fate and toxicity as well as facilitating the biological and medicinal applications of nanomaterials.[10]

The currently accepted paradigm assumes that the formation of NP-protein corona depends upon the physicochemical properties of the NPs (surface charge, coating, shape, roughness, and reactivity), the solvent (*p*H, ionic strength, and temperature), and the proteins (amphiphilicity, charge, p*Ka*, chemical composition, and folding dynamics).[10–12] In addition, plasma proteins may exhibit short ("soft") or long-term ("hard") residence times on their NP substrates,[13] derived from the cooperativity (the Vroman effect,[14] folding/unfolding) between the proteins convolved with the protein affinity for the NP substrates mediated by electrostatic and hydrophobic interactions, *van der Waals* forces, and hydrogen bonding.

In consideration of the vast biological and medicinal potentials of carbon-based nanomaterials, we have examined in the current study the binding of both single-walled and multi-walled CNTs (SWNTs and MWNTs) with fibrinogen (FBI), a major class of plasma glycoprotein that is essential for the coagulation of blood. It is shown through this study that the formation and stability of CNT-FBI coronas correlate with the differential surface areas of the two types of CNTs, as indicated by our UV-vis spectrophotometry and electron and fluorescence measurements. In addition, we have determined that the binding of fluorescently labeled FBI onto CNTs induced static (and possibly dark) quenching of the protein fluorescence. Utilizing the energy transfer between labeled FBI and CNTs (Fig. 1, left panel scheme), we have shown that CNT-FBI coronas could dissociate upon cell translocation, likely as a result of the different affinities of the proteins and the nanostructures for the membrane bilayers. The knowledge derived from this biophysical study complements the existing proteomic, thermodynamic, and chromatographic studies of NP-protein corona,[10,12,13,15–17] and may benefit both *in vitro* and *in vivo* evaluations of biological responses to intentionally administered or accidentally released nanomaterials.

SWNTs (diameter: 1.4 nm, length: 0.5–3 μm, 5% impurities) and MWNTs (OD: 40–70 nm, ID: 5–40 nm, length: 0.5–2 μm) were purchased from Carbon Nanotechnologies and Sigma. Bovine plasma FBI (termed as "unlabeled FBI,", MW: 330 kDa) and Alexa Fluor 546-labeled human plasma FBI (termed as "labeled FBI," ~15 dyes per FBI, Ex/Em: 558/573 nm) were received from Sigma and Invitrogen. The surface areas of SWNTs and MWNTs (in powder form) were derived from the Brunauer-Emmett-Teller (BET) equation[18] and the Barrett-Joyner-Halenda (BJH) method[19] as 855 and 104 m^2/g, respectively, using a physisorption analyzer (Micromeritics ASAP 2010).

a)Electronic mail: pcke11@clemson.edu.

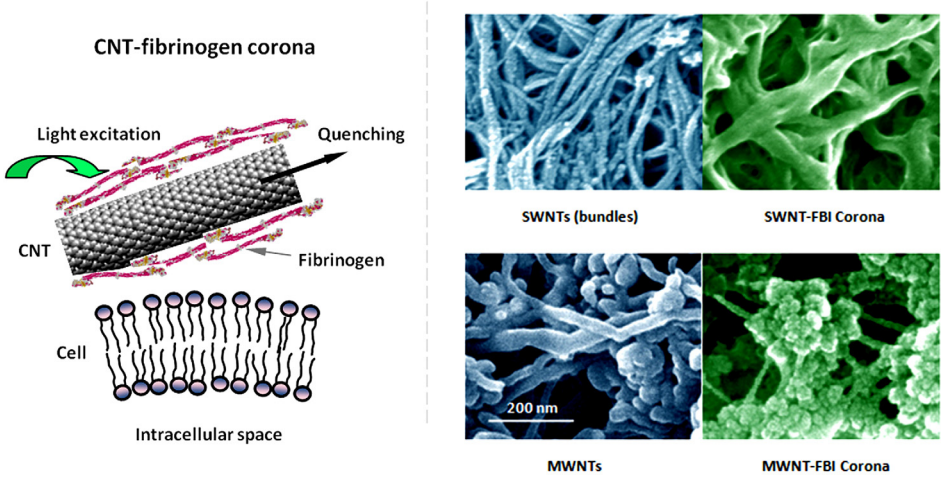

FIG. 1. (Left panel) Schematic of the present study, showing quenching of FBI fluorescence as a result of energy transfer from the proteins to their CNT substrate and translocation of CNT-FBI across a cell membrane. (Right panel) SEM images of SWNT bundles, SWNT-FBI coronas (top panels), MWNTs, and MWNT-FBI coronas (bottom panels). Scale bar: 200 nm for all panels.

The formation of CNT-FBI coronas was first visualized by scanning electron microscopy (SEM) imaging (Fig. 1, right panels). Specifically, CNTs and unlabeled FBI were mixed with Milli-Q water to final concentrations of 0.3 and 0.4 mg/ml, respectively, and incubated overnight. The CNT-FBI samples were then deposited onto aluminum substrates and air-dried. A Hummer 6.2 (Anatech) sputter was used to pre-coat the samples with a 2–4 nm layer of platinum for 1 min (pressure: 80 milli-Torr, voltage: 15 mA). SEM imaging of the CNT-FBI protein coronas was then performed using a Hitachi S4800 electron microscope, at accelerating voltages of 10–15 kV. FBI coated both the SWNTs and MWNTs fully, and especially in the case of MWNTs the protein agglomeration on the nanotube surfaces appeared complex in morphology. This is likely due to the bundling of the SWNTs (Fig. 1, SWNTs control), whose surface roughness and grooves could promote the predominantly axial orientations of the tubular FBI. In comparison, the larger and flatter MWNT surfaces should be less restrictive for the binding of the protein.

The stabilities of the CNT-FBI coronas were characterized by a Cary 300 BIO spectrophotometer (Varian). SWNTs and MWNTs were mixed separately with unlabeled FBI in Milli-Q water (*p*H 6.5) to render final concentrations of 0.5 mg/ml for both types of the CNTs and 2.5 mg/ml for the protein, respectively. The absorbance of the CNT-FBI mixtures was measured at 280 nm, corresponding to the wavelength where the tryptophan residues in FBI exhibited a peak absorbance. The absorbance measurement was conducted for 10 h, at a time interval of 30 min. As shown in Fig. 2(a), the absorbance dropped exponentially until stabilized after ~400 min for the SWNT-FBI sample, while it remained very stable for the MWNT-FBI sample over the entire course of 10 h. This result suggests that the SWNT-FBI coronas were "softer" than the MWNT-FBI, a proposition also corroborated by our analysis below. In addition to *van der Waals* force, hydrophobic interaction, as well as pi-stacking which could underlie the formation of CNT-FBI coronas, FBI could also initiate hydrogen bonding between adjacent CNT-FBI coronas. In the case of SWNTs, such inter-corona interaction could further destabilize the protein coating to induce precipitation.

The two different trends of protein absorbance in Fig. 2(a) can be analyzed using the Mason-Weaver differential equation:[20] $\frac{\partial c}{\partial t} = D\frac{\partial^2 c}{\partial t^2} + sg\frac{\partial c}{\partial z}$, where c is concentration of the solute (i.e., the CNT-FBI corona), D and s are the solute diffusion constant and sedimentation coefficient, z is a length parameter, and g is the acceleration of gravity. Based on the fitted exponents of −0.007 (for SWNTs) and 0 (for MWNTs) in Fig. 2(a), the value of $4D/(sg)^2$ was calculated as 136.7 min for SWNTs and infinity for MWNTs. Assuming m_0 and m_b are the actual and buoyant mass of the solute, ρ_f and ρ_0 the densities of the solute and water, k_b the Boltzmann constant, and T the temperature, and evoking equations $m_b = m_0(1 - \rho_f/\rho_0)$ and $s/D = m_b/k_bT$ derived from the Einstein relation, we estimate that SWNT-FBI possessed an effective density of 1.36 g/cm^3 while MWNT-FBI assumed an effective density approximately equal to that of water. Since the density of SWNTs is ~1.4 times that of water[21] and is only slightly higher than that of SWNT-FBI, we conclude that SWNT bundles were coated with thin layers of FBI to elicit a poor stability in water. In contrast, our analysis implies that MWNTs were adsorbed with multilayers of the protein to render a hard corona.

Fluorescence spectroscopy was utilized to yield more insight on the binding of CNTs and FBI. Specifically, 3 mg of SWNTs and MWNTs were each added to 3 ml of Milli-Q water and bath sonicated for 1 h. The CNTs were then mixed individually with 66.7 μl of the labeled-FBI (1.5 mg/ml) and Milli-Q water to yield samples containing 10–80 μg/ml of SWNTs, 100–800 μg/ml of MWNTs, and 100 μg/ml of labeled FBI. The CNT-labeled FBI samples were then bath sonicated (Precision, Thermo) for 15 min and incubated for 1 h on a rotator. After that, the CNT-labeled FBI mixtures were centrifuged at 12 100 RCF (13 400 rpm) for 15 min and supernatants containing free, labeled FBI molecules were collected. Fluorescence intensities (Ex/Em: 558 nm/565–585 nm) of the supernatants were acquired using a Cary Eclipse spectrofluorometer (Varian).

Compared with the control, the fluorescence intensities of all CNT-labeled FBI samples decreased (Fig. 2(b)) as a result of CNT-FBI corona formation. Such fluorescence quenching can be attributed to the energy transfer between the labeled FBI (donor) upon excitation and the CNTs (acceptor) upon their binding with the proteins. This energy transfer was efficient for SWNTs because their second van Hove absorption transitions (i.e., 500–900 nm)[22,23] coincided

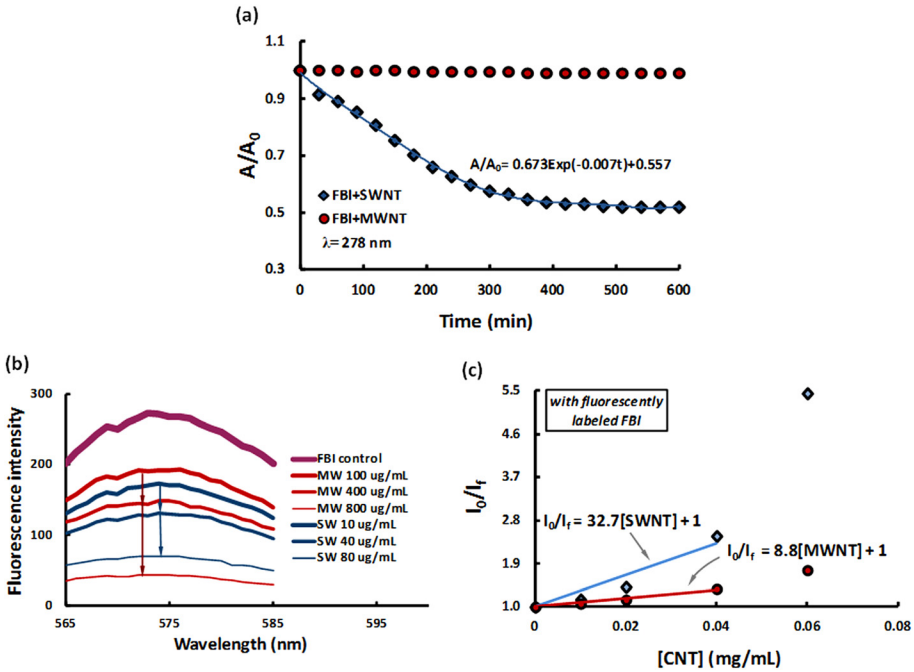

FIG. 2. (a) Normalized absorbance curves showing the stability of CNT-FBI coronas for both SWNTs (blue diamonds) and MWNTs (red circles) over 10 h. (b) Fluorescence intensities of free, labeled FBI supernatants obtained from pelleting SWNT-FBI (blue curves, 10, 40, and 80 μg/ml of the SWNTs) and MWNT-FBI coronas (red curves, 100, 400, and 800 μg/ml of the MWNTs). The fluorescence intensities decreased with increased nanotube concentration for both samples. (c) Stern-Volmer plots show quenching coefficients of 32.7 and 8.8 for SWNT-FBI and MWNT-FBI coronas, respectively. I_0 and I_f: fluorescence intensities of the labeled FBI control and the CNT-labeled FBI mixture, respectively. CNT concentrations: 0.02 to 0.08 mg/ml.

with the emission of the Alexa Fluor 546 dye. Based on geometrical argument and our surface area measurement, the adsorbing capability of SWNTs was estimated as one order of magnitude higher than that of MWNTs per unit mass. Indeed, the fluorescence intensities were comparable between SWNT and the 10× more concentrated MWNT samples, showing a good correlation between protein adsorption capacity and surface area of the CNTs.

The peak fluorescence intensities at 572 nm were plotted for the CNT-labeled FBI samples and fitted using the Stern-Volmer equation:[24] $I_0/I_f = 1 + K_{SV}[CNT]$, here I_0 and I_f are the fluorescence intensities of the labeled FBI (control) and CNT-labeled FBI mixture, respectively, K_{SV} is the Stern-Volmer quenching coefficient, and $[CNT]$ is the concentration of the nanotubes. The Stern-Volmer plots appeared linear for both SWNT-FBI and MWNT-FBI samples at lower CNT concentrations (first 4 data points in Fig. 2(c)), indicating a single quenching mechanism. At higher CNT concentrations, however, both curves deviated from linearity to denote occurrence of additional quenching mechanisms. Since collision between CNTs and FBI should occur more frequently at high concentrations, the linear Stern-Volmer plots at the low CNT concentrations were attributed to static quenching. Though not substantiated in this study CNTs may also absorb light analogously to blackbody.[25] In our experiment, the molar mass ratio of the SWNTs to MWNTs was 1:418, and therefore the ratio of the Stern-Volmer coefficients for the SWNT-FBI and MWNT-FBI samples was $32.7:(8.8 \times 418) = 1:112$. This analysis revealed that MWNTs were far more efficient quenchers than SWNTs, whose smaller diameter and greater curvature were less favorable for the adsorption and alignment of the tubular FBI molecules.

The fluorescence quenching upon corona formation was utilized to examine the stability of CNT-FBI *in vitro*. For this purpose, HT-29 human colonic adenocarcinoma cell lines were cultured in DMEM with 1% penicillin streptomycin, 1% sodium pyruvate, and 10% fetal bovine serum. Approximately 5000 cells were seeded in each well of a chambered glass slide and allowed to attach overnight at 37 °C with 5% CO_2. The culture medium was then replaced with phosphate buffered saline (PBS) and CNTs coated with purified labeled FBI (free proteins removed by centrifugation) and added in each well to obtain concentrations of 1.25 and 12.5 μg/ml for the SWNTs and the MWNTs, respectively. This mass concentration ratio of 1:10 was to ensure the same amount of labeled FBI coated on the two types of nanotubes. The CNT-FBI coronas were allowed to incubate with cells for 2 h, followed by washing and replacing with fresh PBS prior to imaging.

As shown in Fig. 3, the FBI fluorescence is largely quenched in both panels (c) and (d), indicating CNT-FBI corona formation for both SWNTs and MWNTs. Cell adsorption of SWNT-FBI and fluorescence recovery of FBI in intracellular space were evident (Fig. 3(e), arrows), suggesting dissociation of SWNTs and FBI post membrane translocation. The isoelectric point of FBI is 5.5,[27] and therefore the proteins were slightly positively charged when stored/processed in endosomes and lysosomes (~*p*H 4.5) and slightly negatively charged when located in cytosol (~*p*H 7.2). Since the SWNT surfaces were charge neutral, changes in *p*H in the intra- and extracellular environment should not drastically impact the binding of SWNT-FBI. The dissociation of SWNTs and FBI is therefore attributed to their differential affinities for the amphiphilic cell membranes.

Pronounced cell adsorption of MWNT-FBI and recovery of FBI fluorescence in the extracellular space were observed, but minimal fluorescence was seen in the intracellular space perhaps due to the high energy cost for MWNT endocytosis (Fig. 3(f)). In addition, cell damage (from elongated to round shapes) was more apparent for MWNTs than SWNTs (Figs. 3(f) vs. 3(e)), likely due to the higher dosage and the toxicity associated with the MWNTs.[26]

In short, we have examined the formation and stability of CNT-FBI coronas in the aqueous phase and *in vitro*. The binding between CNTs and FBI is consistent with the high hydrophobic and aromatic moieties of both the protein and the

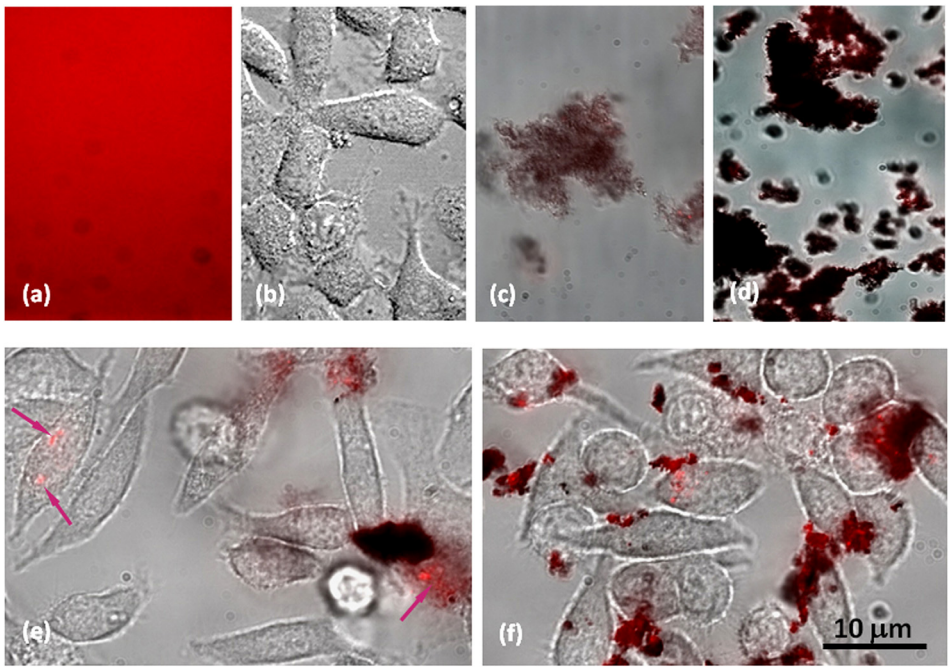

FIG. 3. HT-29 cell uptake of CNT-FBI coronas overlaid from bright field and confocal fluorescence images. (a) and (b) Controls of labeled FBI fluorescence and HT-29 cells. (c) and (d) Controls of SWNT-FBI and MWNT-FBI showing fluorescence quenching. (e) Cell adsorption of SWNT-FBI and FBI fluorescence recovery in the intracellular space (arrows). (f) Pronounced cell adsorption and dissociation of MWNT-FBI in the extracellular space indicated by fluorescence recovery. Cell damage induced by MWNTs is evident. Scale bar: 10 μm for all images.

nanotubes, and agrees with the *in silico* studies involving similar systems.[28–30] The differential "hardness" and stability of the SWNT-FBI and MWNT-FBI coronas were analyzed based on the concept of buoyant mass and Stern-Volmer plots, and were attributed to the different surface areas and morphology of the two types of CNTs. This study offers a new biophysical perspective for elucidating the concept of NP-protein corona, a topic essential to our understanding of the implications and applications of nanomaterials in living systems.

This work was supported by NSF CAREER Award CBET-0744040 and NSF Grant CBET-1232724 to Ke and NIEHS Grant R01 ES019311 02S1 to Brown and Ke. The authors thank Mr. Onur Guven Apul and Dr. Tanju Karanfil for their assistance with surface area measurement of the carbon nanotubes.

[1]D. Pantarotto, C. D. Partidos, R. Graff, J. Hoebeke, J.-P. Briand, M. Prato, and A. Bianco, J. Am. Chem. Soc. **125**, 6160 (2003).
[2]A. E. Nel, L. Madler, D. Velegol, T. Xia, E. M. V. Hoek, P. Somasundaran, F. Klaessig, V. Castranova, and M. Thompson, Nature Mater. **8**, 543 (2009).
[3]P. C. Ke and M. H. Lamm, Phys. Chem. Chem. Phys. **13**, 7273 (2011).
[4]J. L. Bahr and J. M. Tour, J. Mater. Chem. **12**, 1952 (2002).
[5]R. J. Chen, Y. Zhang, D. Wang, and H. J. Dai, J. Am. Chem. Soc. **123**, 3838 (2001).
[6]M. Zheng, A. Jagota, E. D. Semke, B. A. Diner, R. S. McLean, S. R. Lustig, R. E. Richardson, and N. G. Tassi, Nature Mater. **2**, 338 (2003).
[7]R. Rao, J. Lee, Q. Lu, G. Keskar, K. O. Freedman, W. C. Floyd, A. M. Rao, and P. C. Ke, Appl. Phys. Lett. **85**, 4228 (2004).
[8]Y. Wu, J. S. Hudson, Q. Lu, J. M. Moore, A. S. Mount, A. M. Rao, E. Alexov, and P. C. Ke, J. Phys. Chem. B **110**, 2475 (2006).
[9]I. Lynch, A. Salvati, and K. A. Dawson, Nat. Nanotechnol. **4**, 546 (2009).
[10]A. A. Shemetov, I. Nabiev, and A. Sukhanova, ACS Nano **6**, 4585 (2012).
[11]I. Lynch and K. A. Dawson, Nano Today **3**, 40 (2008).
[12]M. Mahmoudi and V. Serpooshan, J. Phys. Chem. C. **115**, 18275 (2011).
[13]S. Milani, F. B. Bombelli, A. S. Pitek, K. A. Dawson, and J. Rädler, ACS Nano **6**, 2532 (2012).
[14]L. Vroman, A. L. Adams, G. C. Fischer, and P. C. Munoz, Blood **55**, 156 (1980).
[15]J. Sund, H. Alenius, M. Vippola, K. Savolainen, and A. Puustinen, ACS Nano **5**, 4300 (2011).
[16]T. Cedervall, I. Lynch, S. Lindman, T. Berggard, E. Thulin, H. Nilsson, K. A. Dawson, and S. Linse, Proc. Natl. Acad. Sci. U.S.A. **104**, 2050 (2007).
[17]J. Wang, U. B. Jensen, G. V. Jensen, S. Shipovskov, V. S. Balakrishnan, D. Otzen, J. S. Pedersen, F. Besenbacher, and D. S. Sutherland, Nano Lett. **11**, 4985 (2011).
[18]S. Brunauer, P. H. Emmett, and E. Teller, J. Am. Chem. Soc. **60**, 309 (1938).
[19]E. P. Barrett, L. G. Joyner, and P. P. Halenda, J. Am. Chem. Soc. **73**, 373 (1951).
[20]M. Mason and W. Weaver, Phys. Rev. **23**, 412 (1924).
[21]G. Guo, T. Cagin, and W. A. Goddard III, Nanotechnology **9**, 184 (1998).
[22]S. M. Bachilo, M. S. Strano, C. Kittrell, R. H. Hauge, R. E. Smalley, and R. B. Weisman, Science **298**, 2361 (2002).
[23]S. Lin, G. Keskar, Y. Wu, X. Wang, A. S. Mount, S. J. Klaine, J. M. Moore, A. M. Rao, and P. C. Ke, Appl. Phys. Lett. **89**, 143118 (2006).
[24]O. Stern and M. Volmer, Physik. Zeitschr. **20**, 183 (1919).
[25]K. Mizuno, J. Ishii, H. Kishida, Y. Hayamizu, S. Yasuda, D. N. Futaba, M. Yumura, and K. Hata, Proc. Natl. Acad. Sci. U.S.A. **106**, 6044 (2009).
[26]C. A. Poland, R. Duffin, I. Kinloch, A. Maynard, W. A. H. Wallace, A. Seaton, V. Stone, S. Brown, W. MacNee, and K. Donaldson, Nat. Nanotechnol. **3**, 423 (2008).
[27]E. A. Caspary and R. A. Kekwick, Biochem. J. **67**, 41 (1957).
[28]C. Ge, J. Du, L. Zhao, L. Wang, Y. Liu, D. Li, Y. Yang, R. Zhou, Y. Zhao, Z. Chai, and C. Chen, Proc. Natl. Acad. Sci. U.S.A. **108**, 16968 (2011).
[29]S. Vaitheeswaran and A. E. Garcia, J. Chem. Phys. **134**, 125101 (2011).
[30]A. K. Jana and N. Sengupta, Biophys. J. **102**, 1889 (2012).